# Imidazole Complexes of Low-Spin Iron(III) Porphyrin π-Cation Radical Species. Models for the Compound I π-Cation Radical State of Peroxidases

**Harold M. Goff* and Martin A. Phillippi**

*Contribution from the Department of Chemistry, University of Iowa, Iowa City, Iowa 52242.*
*Received November 8, 1982*

**Abstract:** Addition of imidazole to methylene chloride solutions of the previously characterized iron(III) porphyrin π-cation radicals permits generation of new oxidized imidazole complexes. These transient paramagnetic bis(imidazole) complexes have been characterized in solution by low-temperature proton NMR measurements. Oxidized iron tetraphenylporphyrin derivatives exhibit large, alternating upfield and downfield phenyl proton chemical shifts, which are reminiscent of the parent iron(III) porphyrin radical. A far upfield pyrrole proton NMR signal resembles that of the low-spin iron(III) complex in both shift direction and line width. The oxidized imidazole complexes are thus best described as low-spin iron(III) porphyrin π-cation radicals. Magnetic moment estimates of 2.8 and 3.3 $\mu_B$ for a tetraphenylporphyrin derivative and octaethylporphyrin, respectively, indicate that metal and radical spins do not strongly couple. The proton NMR spectrum of the oxidized bis(imidazole)iron(III) etioporphyrin complex resembles that of horseradish peroxidase compound I in that a relatively sharp ring methyl signal is found in a far downfield position.

## Introduction

Generation of highly oxidized iron porphyrin complexes has recently been a major goal of several research groups.[1-15] Aside from the novelty of such "iron(IV)" species, these reactive intermediates may have practical value as active oxidizing agents for catalytic functionalization of saturated hydrocarbons.[7,16-18] Further rationale for synthetic and physical studies is found in the appearance of putative iron(IV) states as intermediates in the redox cycle of certain hemoproteins.[19-22] Horseradish peroxidase (HRP) constitutes the best-characterized example of these high oxidation state enzymes. The resting high-spin iron(III) porphyrin prosthetic group undergoes a two-electron oxidation upon interactions with hydrogen peroxide or organic peroxides. The resulting green species has been labeled as compound I. On the basis of visible,[23] Mössbauer,[24,25] ESR,[25] and ENDOR[26] spectral measurements, HRP compound I is best described as a low-spin iron(IV) porphyrin π-cation radical.

$$PFe^{III} + H_2O_2 \rightarrow \cdot PFe^{IV}{=}O + H_2O \qquad (1)$$

One-electron reduction of compound I yields the red species compound II.

$$\cdot PFe^{IV}{=}O + R \rightarrow PFe^{IV}{=}O + R^+ \qquad (2)$$

Presence of a ferryl or hydroxyl group is inferred from kinetic studies and model compound work. An imidazole (histidine) residue provides an axial ligand in the resting enzyme, and it is generally assumed that this ligand is present throughout the catalytic cycle.[20,21]

One-electron oxidation of isolated iron(III) porphyrin complexes can in principle yield either an iron(IV) species or an iron(III) porphyrin π-cation radical. Although it was first assumed that electrochemical oxidation of high-spin chloroiron(III) porphyrins produced iron(IV) complexes,[2] various physical measurements now demonstrate the existence of stable iron(III) porphyrin π-cation radicals,[5,6,8-10,12-15] Equivalent species can be generated via electrochemical methods[2,3,5,8,10,12,15] and by chemical oxidation using organic free radical reagents,[6,8,9,13,27] an iodine–silver salt

(1) Wolberg, A.; Manassen, J. *J. Am. Chem. Soc.* **1970**, *92*, 2982–2991.
(2) (a) Felton, R. H.; Owen, G. S.; Dolphin, D.; Fajer, J. *J. Am. Chem. Soc.* **1971**, *93*, 6332–6334. (b) Felton, R. H.; Owen, G. S.; Dolphin, D.; Forman, A.; Borg, D. C.; Fajer, J. *Ann. N. Y. Acad. Sci.* **1973**, *206*, 504–514.
(3) Phillippi, M. A.; Goff, H. M. *J. Am. Chem. Soc.* **1979**, *101*, 7641–7643.
(4) (a) Chin, D. H.; Balch, A. L.; La Mar, G. N. *J. Am. Chem. Soc.* **1980**, 102, 1446–1448. (b) Chin, D. H.; La Mar, G. N.; Balch, A. L. *Ibid.*, 4344–4350. (c) *Ibid.*, 5945–5947.
(5) Phillippi, M. A.; Shimomura, E. T.; Goff, H. M. *Inorg. Chem.* **1981**, *20*, 1322–1325.
(6) Gans, P.; Marchon, J.-C.; Reed, C. A.; Regnard, J.-R. *Nouv. J. Chim* **1981**, 203–204.
(7) Groves, J. T.; Haushalter, R. C.; Nakamura, M.; Nemo, T. E.; Evans, B. J. *J. Am. Chem. Soc.* **1981**, *103*, 2884–2886.
(8) Shimomura, E. T.; Phillippi, M. A.; Goff, H. M.; Scholz, W. F.; Reed, C. A. *J. Am. Chem. Soc.* **1981**, *103*, 6778–6780.
(9) Reed, C. A. In "Electrochemical and Spectrochemical Studies of Biological Redox Components"; Kadish, K. M., Ed.; American Chemical Society: Washington, DC, 1982; Adv. Chem. Ser. No. 201, pp 333–356 and references therein.
(10) Goff, H. M.; Phillippi, M. A. Boersma, A. D.; Hansen, A. P. In "Electrochemical and Spectrochemical Studies of Biological Redox Components", Kadish, K. M., Ed.; American Chemical Society: Washington DC, 1982; Adv, Chem. Ser. No. 201, pp 357–376.
(11) Simonneaux, G.; Scholz, W. F.; Reed, C. A.; Lang, G. *Biochim. Biophys. Acta* **1982**, *716*, 1–7.
(12) Phillippi, M. A.; Goff, H. M. *J. Am. Chem. Soc.* **1982**, *104*, 6026–6034.
(13) Scholz, W. F.; Reed, C. A.; Lee, J. Y.; Scheidt, W. R.; Lang, G. *J. Am. Chem. Soc.* **1982**, *104*, 6791–6793.
(14) Buisson, G.; Deronzier, A.; Duee, E.; Gans, P.; Marchon, J.-C.; Regnard, J.-R. *J. Am. Chem. Soc.* **1982**, *104*, 6793–6796.
(15) Boersma, A. D.; Goff, H. M. *Inorg. Chem.*, in press.
(16) (a) Groves, J. T.; Nemo, T. E.; Myers, R. S. *J. Am. Chem. Soc.* **1979**, *101*, 1032–1033. (b) Groves, J. T.; Kruper, W. J.; Nemo, T. E.; Myers, R. S. *J. Mol. Catal.* **1980**, *7*, 169–177.
(17) Chang, C. K.; Kuo, M.-S. *J. Am. Chem. Soc.* **1979**, *101*, 3413–3415.
(18) Shannon, P.; Bruice, T. C. *J. Am. Chem. Soc.* **1981**, *103*, 4580–4582.
(19) Dunford, H. B.; Stillman, J. S. *Coord. Chem. Rev.* **1976**, *19*, 187–251.
(20) Chang, C. K.; Dolphin, D. In "Bioorganic Chemistry"; Van Tamelen, E. E., Ed.; Academic Press: New York, 1978; Vol. 4, pp 37–80.
(21) Hewson, W. D.; Hager, L. P. In "The Porphyrins"; Dolphin, D., Ed.; Academic Press: New York, 1979; Vol. VII, pp 295–332.
(22) Hanson, L. K.; Chang, C. K.; Davis, M. S.; Fajer, J. *J. Am. Chem. Soc.* **1981**, *103*, 663–670.
(23) (a) Dolphin, D.; Felton, R. H. *Acc. Chem. Res.* **1974**, *7*, 26–32. (b) Dolphin, D.; Addison, A. W.; Cairns, M.; Dinello, R. K.; Farrell, N. P.; James, B. R.; Paulson, D. R.; Welborn, C. *Int. J. Quantum Chem.* **1979**, *16*, 311–329.
(24) (a) Moss, T. H.; Ehrenberg, A.; Bearden, A. J. *Biochemistry* **1969**, *8*, 4159–4162. (b) Harami, T.; Maeda, Y.; Morita, Y.; Trautwein, A.; Gonser, U. *J. Chem. Phys.* **1977**, *67*, 1164–1169.
(25) Schulz, C. E.; Devaney, P. W.; Winkler, H.; Debrunner, P. G.; Doan, N.; Chiang, R.; Rutter, R.; Hager, L. P. *FEBS Lett.* **1979**, 103, 102–105.
(26) Roberts, J. E.; Hoffman, B. M.; Rutter, R.; Hager, L. P. *J. Biol. Chem.* **1981**, *256*, 2118–2121.
(27) Shine, H. J.; Padilla, A. G.; Wu, S.-M. *J. Org. Chem.* **1979**, *44*, 4069–4075.

0002-7863/83/1505-7567$01.50/0 

mixture,[12,27,28] or ferric perchlorate.[14] Physical studies that provide a basis for the porphyrin radical formulation include visible,[23] infrared,[8] NMR,[3,5,6,10,12-15] and Mössbauer[6,9,12-14] spectral measurements, as well as redox potential determinations.[5] Proton NMR spectra are distinctive for iron tetraphenylporphyrin ((TPPFe) radicals of the $a_{2u}$ type. This particular radical exhibits large unpaired spin density at the meso carbon position,[22] and as a consequence, phenyl proton NMR signals are shifted to extreme upfield and downfield positions. Such alternating phenyl shift patterns provide the basis for assigning radical character to the oxidized low-spin bis(imidazole)iron(III) porphyrin complexes described here. These transient species have been generated and characterized in situ at low temperature. Proton NMR studies of the bis(imidazole)iron(III) porphyrin $\pi$-cation radicals provide a better understanding of the corresponding NMR measurements made for HRP compounds I and II.[29,30]

## Experimental Section

Oxidized iron porphyrin complexes were generally obtained via electrochemical preparations as described recently.[12] Controlled potential electrolysis of the appropriate chloroiron(III) porphyrin slightly beyond the first oxidation wave effected nearly complete conversion to the iron(III) porphyrin $\pi$-cation radical. The $\mu$-oxo dimeric iron(III) tetraphenylporphyrin was oxidized in a similar manner at either the first or second oxidation potential.[3,12] These iron(III) porphyrin $\pi$-cation radical chloride perchlorate species and $\mu$-oxo dimeric perchlorate compounds were isolated in the solid state following selective extraction of supporting electrolyte or iron porphyrin by appropriate solvents.[12] Solid materials were weighed into NMR tubes for subsequent dissolution and reaction with imidazole solutions at low temperature.

The iron(III) etioporphyrin I((ETIO)Fe) and iron(III) tetrakis-(2,4,6-trimethoxyphenyl)porphyrin $\pi$-cation radicals were generated in situ by oxidation of the parent chloroiron(III) complex with 1 equiv of the doubly oxidized dimer $((TPP)Fe)_2O(ClO_4)_2$.[3] The tetrakis(2,4,6-trimethoxyphenyl)porphyrin [TPP(2,4,6-$OCH_2$)] was prepared by condensation of the aldehyde and pyrrole as previously described.[31] Meso-deuterated octaethylporphyrin (OEP) was prepared by toluenesulfonic acid-$d_1$ exchange.[32] Imidazole was purified by repeated recrystallization from benzene, followed by vacuum drying. Deuterated methylene chloride was dried over activated 3-Å molecular sieves prior to dissolution of oxidized materials.

Imidazole adducts of iron(III) porphyrin radical species were prepared in situ in NMR tubes at low temperature. The solid material was first dissolved in $CD_2Cl_2$ at ambient temperature and the nitrogen-flushed tube was sealed with a septum cap. The NMR tube was immersed almost completely in powdered dry ice, and a small amount of 0.1 M imidazole in $CD_2Cl_2$ or $CDCl_3$ was injected by syringe. The drop of titrant was allowed to run down the wall of the cold NMR tube before making contact with the bulk solution. A quick inversion of the tube prior to insertion into the cold NMR probe was sufficient to promote mixing. The solution was allowed to equilibrate to the NMR probe temperature before the spectrum was recorded.

Proton NMR spectra were obtained at 90 MHz with pulsed Fourier transform Bruker HX-90E or JEOL FX-90Q spectrometers. Temperature calibration was performed by the methanol thermometer method.[33] Complete NMR spectra were recorded for solutions used to measure magnetic susceptibility by the Evans method.[34] Density corrections for $CD_2Cl_2$ at low temperature were made by using the empirical function for $CHCl_3$.[35] Diamagnetic corrections were based on the reported value for the free ligand.[36]

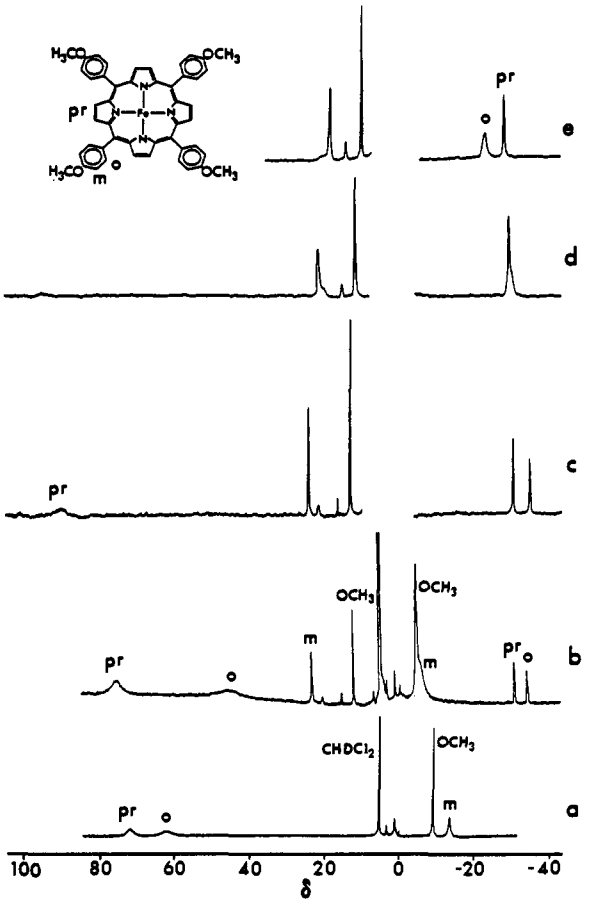


**Figure 1.** Proton NMR spectra for the titration of $(TPP(p\text{-}OCH_3))FeCl(ClO_4)$ with imidazole: −38 °C, $CD_2Cl_2$ solvent, 0.01 M iron porphyrin, chemical shifts with respect to internal $(CH_3)_4Si$. Imidazole added: (a) 0.0 equiv; (b) 0.5 equiv; (c) 1.0 equiv; (d) 1.5 equiv; (e) 2.0 equiv.

## Results

**Iron Tetraphenylporphyrin Derivatives.** Attempts to electrochemically oxidize bis(imidazole)iron(III) porphyrins at ambient temperature were unsuccessful. Cyclic voltammograms of the low-spin iron(III) complex revealed highly irreversible anodic waves ($CH_2Cl_2$ solvent, 0.1 M tetrabutylammonium perchlorate media). Likewise, addition of imidazole to $CH_2Cl_2$ solutions of iron(III) porphyrin radical species brought immediate reduction at ambient temperature. It was found, however, that careful addition of imidazole to solutions of the oxidized compounds at dry ice temperatures caused only partial reduction and produced a new adduct which was sufficiently stable to observe by proton NMR spectroscopy.

Results of a titration experiment at −38 °C are shown in Figure 1. The tetrakis(*p*-methoxyphenyl)porphyrin (TPP(*p*-$OCH_3$)) was utilized extensively due to a less anodic oxidation potential and enhanced stability as compared with unsubstituted TPP.[12] The proton spectrum of $(TPP(p\text{-}OCH_3))FeCl(ClO_4)$ is shown in Figure 1a. Peak assignments have been made previously.[12] Phenyl resonances clearly show an alternating radical-like shift pattern in that the *o*-proton signal is far downfield and the *m*-proton and *p*-$OCH_3$ signals are shifted appreciably upfield (the *p*-proton signal of the unsubstituted TPP derivative is also far downfield). Addition of imidazole to the high-spin iron(III) porphyrin radical species at low temperature induces partial reduction of the radical. This is evident in migration of the pyrrole proton signal in Figure 1a–c from 73 to 92 ppm (the pyrrole resonance for the iron(III) porphyrin at −38 °C is at 98 ppm). The phenyl resonances of the radical species also move toward the positions expected for the simple high-spin iron(III) complex. Observation of only averaged signals for high-spin iron(III) porphyrin and high-spin iron(III) porphyrin radical derivatives is fully consistent with rapid

(28) Kadish, K. M.; Rhodes, R. K.; Bottomley, L. A.; Goff, H. M. *Inorg. Chem.* **1981**, *20*, 3195–3200.
(29) (a) Morishima, I.; Ogawa, S. *J. Am. Chem. Soc.* **1978**, *100*, 7125–7127. (b) Morishima, I., Ogawa, S. *Biochem. Biophys. Res. Commun.* **1978**, *83*, 946–953. (c) Morishima, I.; Ogawa, S. *Biochemistry* **1978**, *17*, 4384–4388.
(30) (a) La Mar G. N.; de Ropp, J. S. *J. Am. Chem. Soc.* **1980**, *102*, 395–397. (b) La Mar, G. N.; de Ropp, J. S.; Smith, K. M.; Langry, K. C. *J. Biol. Chem.* **1981**, *256*, 237–243.
(31) Vaska, L.; Amundsen, A. R.; Brady, R.; Flynn, B. R.; Nakai, H. *Finn. Chem. Lett.* **1974**, 66–69.
(32) Smith, K. M.; Langry, K. C.; de Ropp, J. S. *J. Chem. Soc., Chem. Commun.* **1979**, 1001–1003.
(33) Van Geet, A. L. *Anal. Chem.* **1968**, *40*, 2227–2229.
(34) Evans, D. F. *J. Chem. Soc.* **1959**, 2003–2005.
(35) "International Critical Tables"; Washburn, E. W., Ed.; McGaw-Hill: New York, 1928; Vol. 3, p 27.
(36) Eaton, S. S.; Eaton, G. R. *Inorg. Chem.* **1980**, *19*, 1095–1096.

Table I. Proton NMR Resonances for Bis(imidazole)iron(III) Porphyrin Radicals[a]

| proton | TPP-($p$-$OCH_3$)[b] | TPP[b] | TPP-(2,4,6-$OCH_3$)[c] | OEP[d] | ETIO[d] |
|---|---|---|---|---|---|
| pyrrole | −32.7 | −40.1 | −40.4 | | |
| $o$-phenyl | −36.3 | −31.7 | | | |
| $m$-phenyl | 24.8 | 30.4 | 26.7 | | |
| $p$-phenyl | | −22.1 | | | |
| $p$-$OCH_3$ | 12.9 | | 9.5 | | |
| $o$-$OCH_3$ | | | 12.8 | | |
| ring $CH_2$ | | | | 51.7 | 50.4 |
| ring $CH_3$ | | | | | 133.1 |

[a] $CD_2Cl_2$ solvent, 0.01 M iron porphyrin, 0.5 equivalent-of imidazole, referenced to $(CH_3)_4Si$; downfield shifts are given positive sign. [b] −38 °C. [c] −30 °C, 1.0 equivalent of imidazole present. [d] −51 °C; ethyl-$CH_3$ groups were obscured by the solvent signal; the meso proton signal was not detected.

electron exchange (on the NMR time scale) as has been described previously.[12]

Addition of imidazole is also associated with appearance of new porphyrin signals in both upfield and downfield regions. These are assigned by integrations and by comparison of analogous spectra for the tetrakis(2,4,6-trimethoxyphenyl)porphyrin and unsubstituted tetraphenylporphyrin derivatives. Signals are observed in the 25 to 30 and −32 to −40 ppm region for all three species. The downfield and upfield signals (of equal intensity) must be associated with phenyl meta and pyrrole protons, as these residues are common to all three derivatives. Specific assignments are made by reductive titration with excess imidazole (vide infra) or tetrabutylammonium iodide, in which case the signals for the oxidized imidazole complex migrate to resonance values known for the respective low-spin bis(imidazole)iron(III) porphyrin adduct. On this basis the downfield signal is assigned as the phenyl $m$-proton resonance, and the pyrrole proton signal must be in the upfield region. The two upfield signals in Figure 1b–e are distinguished by reductive titration, in which case it may be seen that the signals cross (Figure 1d) as the contribution from reduced iron porphyrin increases. Greater sensitivity of the phenyl $o$-proton to reduction thus permits its assignment for the (TPP($p$-$OCH_3$))Fe and (TPP)Fe complexes. Signal intensities provide ready assignment of phenyl $p$-proton and methoxy resonances as listed in Table I.

Integration of the far downfield and upfield pyrrole signals in Figure 1b,c indicates a 2:1 stoichiometry for imidazole–iron porphyrin coordination. The small signals at 22.1 and 16.5 ppm appear to be from coordinated imidazole residues, and these signals have approximately one-fourth the integrated area of phenyl ortho and meta and pyrrole proton residues of the imidazole complex. The imidazole signals have not been assigned specifically, but both remained when $N$-deuterated imidazole was employed.

Spectra for the oxidized imidazole complex in Figure 1b,c are essentially the same despite the fact that a larger fraction of the chloroiron species is reduced for spectrum 1c. This indicates that ligand and electron exchange between oxidized imidazole complexes and chloroiron(III) species is slow on the NMR time scale. Effectively this also means that the oxidation potential for the bis(imidazole) complex is lower than that for the high-spin chloro complex. As additional imidazole is added in Figure 1d,e, a considerable amount of the reduced (imidazoleiron(III) complex is generated. This bis(imidazole)iron(III) porphyrin complex is seemingly in rapid electron exchange with the oxidized bis(imidazole) iron porphyrin adduct, as is evident in the migration of phenyl proton resonances toward the diamagnetic region. The pyrrole proton signal of the bis(imidazole) species also exhibits a downfield bias as proportionately more of the mixture is left in the reduced form. At −38 °C the limiting pyrrole proton signal for the bis(imidazole)iron(III) porphyrin is found at −24 ppm. Thus, the oxidized complex exhibits an upfield pyrrole shift some 9–16 ppm greater than the value for the parent low-spin iron(III) species. Overall the shift and line-width pattern of the pyrrole proton signal is reminiscent of the low-spin iron(III) state, and

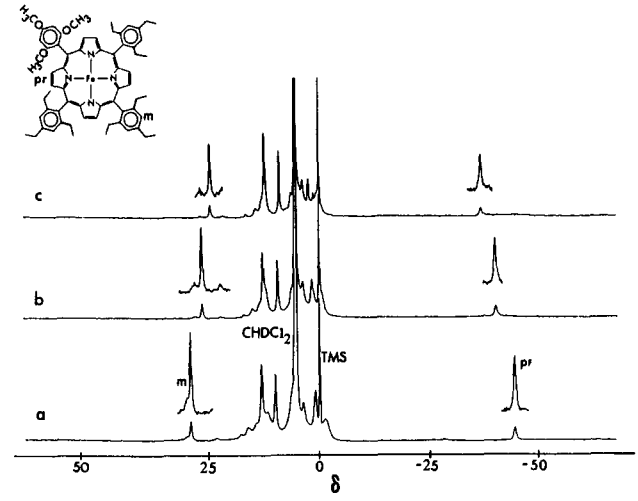


**Figure 2.** Variable temperature proton NMR spectra for (TPP(2,4,6-$OCH_3$))FeCl($ClO_4$) with 1 equiv of imidazole present. The oxidized species was prepared by oxidation with 1 equiv of $((TPP)Fe)_2O(ClO_4)_2$ followed by addition of imidazole. (a) −51 °C; (b) −30 °C; (c) −10 °C.

large, alternating phenyl proton shifts are much like those expected for an aromatic radical. Thus, porphyrin-centered rather than metal-centered oxidation seemingly is maintained for the low-spin state.

Additional notes should be made about practical aspects of generating the low-spin oxidized complex. Variation in line widths for low-spin species in Figure 1 may be due entirely to experimental problems in that any reduction occurring during the several minutes required to collect approximately 1000 transients would give apparent broadening and non-Lorentzian line shapes. Addition of excess imidazole beyond the 2 equiv required for complete coordination serves to reduce the species to the low-spin bis(imidazole)iron(III) complex. Attempts to generate the corresponding oxidized $N$-methylimidazole and pyridine complexes were unsuccessful, as these two ligands brought immediate reduction. This may be due to the lower binding affinity and hence sizeable concentrations of free ligand at equilibrium. Recording low temperature visible spectra of the imidazole complexes presents special problems in that the excess imidazole required to fully ligate the iron center serves as a reducing agent.[37] In the absence of spectra, it should be noted that NMR samples of the oxidized imidazole complexes are decidely green. This color must be contrasted to the red color known for HRP compound II (low-spin iron(IV)) and for simple low-spin bis(imidazole)iron(III) porphyrins.

**Variable Temperature Measurements.** The range over which variable temperature measurements could be made was limited by solubility and stability of the oxidized imidazole complex. Proton NMR measurements were performed in the range from −69 to −38 °C for the (TPP($p$-$OCH_3$))FeCl($ClO_4$) compound to which 2 equiv of imidazole had been added. The plot of pyrrole proton chemical shifts vs. the reciprocal absolute temperature (Curie plot) was reasonably linear and had an intercept near the diamagnetic pyrrole proton value. However, phenyl $o$- and $m$-

(37) The equilibrium constant for imidazole binding to (TPP)FeCl at 25 °C is $\sim 10^6$ $M^{-2}$.[38,39] If a value of $10^8$ $M^{-2}$ is assumed for oxidized (TPP($p$-$OCH_3$))$FeCl^+$ at −40 °C, calculation shows that a concentration of $3 \times 10^{-4}$ M free imidazole is required to maintain 90% of the porphyrin in the bis-ligated form. Concentrations required for spectrophotometric measurements are on the order of $10^{-4}$ M, and thus excess imidazole is available as a reducing agent. Equilibrium constants for $N$-methylimidazole and pyridine are respectively three orders and five orders of magntidue smaller than that for imidazole.[38,39] Thus, even for NMR concentrations of 0.01 M iron porphyrin, sufficient free $N$-methylimidazole and pyridine are potentially available to promote reduction.

(38) Walker, F. A.; Lo, M.-W.; Ree, M. T. *J. Am. Chem. Soc.* **1976**, *98*, 5552–5560.

(39) Satterlee, J. D.; La Mar, G. N.; Frye, J. S. *J. Am. Chem. Soc.* **1976**, *98*, 7275–7282.

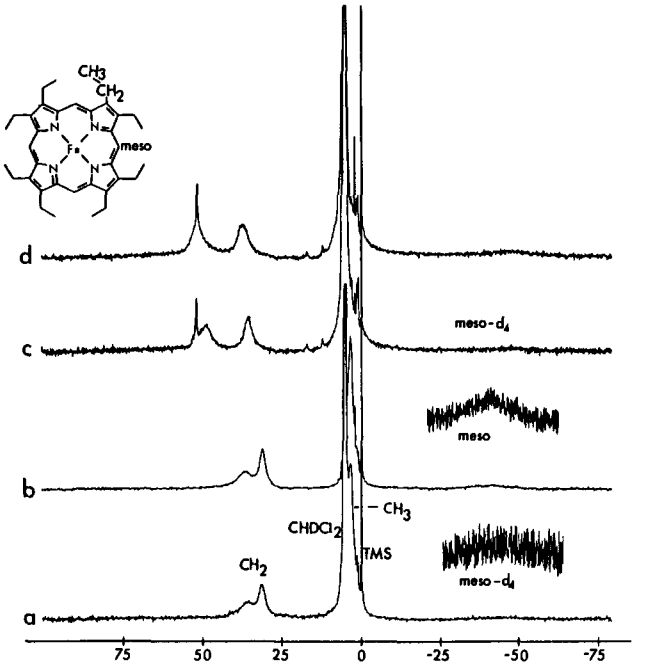


Figure 3. Proton NMR spectra of (OEP)FeCl($ClO_4$) and imidazole adducts: −51 °C, $CD_2Cl_2$ solvent, 0.01 M iron porphyrin. (a) (OEP)-FeCl($ClO_4$)-*meso*-$d_4$; (b) (OEP)FeCl($ClO_4$); (c) 0.5 equiv of imidazole added to (OEP)FeCl($ClO_4$)-*meso*-$d_4$; (d) 0.5 equiv of imidazole added to (OEP)FeCl($ClO_4$).

proton plots for this compound were decidedly nonlinear and had respective intercepts far downfield and far upfield of the aromatic region. The deviations are in the direction expected for partial reduction of the complex between and during acquisition of the higher temperature spectra. A more stable oxidized imidazole complex is generated from the TPP(2,4,6-$OCH_3$) derivative. Proton spectra at three different temperatures are shown in Figure 2. The Curie plot for the pyrrole proton signal was quite linear, and the intercept is only 3 ppm upfield from the diamagnetic pyrrole proton value. The phenyl *m*-proton plot shows some deviation from linearity and the intercept is only slightly upfield. These Curie law deviations are no larger than those seen in bis-(imidazole)iron(III) porphyrin complexes.[40] Overall the well-behaved Curie plots for pyrrole protons of the oxidized complex illustrate that the iron(III) center is magnetically simple over the temperature range examined. This dictates that antiferromagnetic coupling between the iron and radical spins must be small and that mixing of other states must be relatively unimportant.

**Octaethylporphyrin and Etioporphyrin Complexes.** Additon of substoichiometric amounts of imidazole to (OEP)FeCl($ClO_4$) at low temperature yields a new, sharp signal in the 50 ppm region. The oxidized imidazole complex is considerably more reactive than that generated from TPP derivatives. This is apparent in Figure 3 in that only 0.5 equiv of imidazole brings about considerable reduction of the high-spin iron(III) porphyrin radical. In this instance the broad ring-$CH_2$ signals move further downfield as the radical is partially reduced in Figure 3c. Use of meso-deuterated (OEP)FeCl($ClO_4$) demonstrates that the sharp 50 ppm signal is not that of the meso proton, and the resonance is thus assigned to the ring-$CH_2$ residues. Small differences between Figure 3, parts c and d, may be ascribed to variable amounts of reduction, depending on subtle differences in mixing procedure. Lack of splitting in the 50 ppm signal is a strong indication that the complex has two identical axial ligands and that the iron lies in the plane of the prophyrin. The meso signal of the oxidized imidazole complex has not been located and is presumably broadened beyond detection or is obscured in the diamagnetic region. The methyl signal apparently lies under the solvent signal.

(40) La Mar, G. N.; Walker, F. A. *J. Am. Chem. Soc.* **1973**, *95*, 1782–1790.

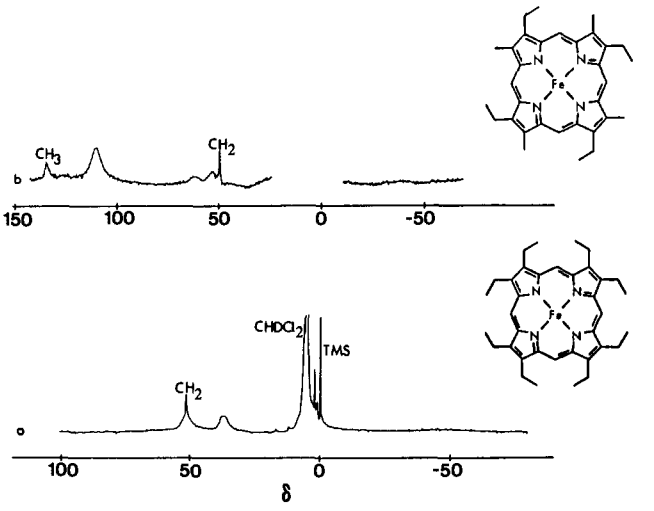


Figure 4. Proton NMR spectra of oxidized (OEP)Fe and (ETIO)Fe imidazole complexes: −51 °C, $CD_2Cl_2$ solvent, 0.01 M iron porphyrin. (a) (OEP)FeCl($ClO_4$) with 0.5 equiv of imidazole added; (b) (ETIO)-FeCl($ClO_4$) with 0.5 equiv of imidazole added. The oxidized species was generated in situ by addition of 1 equiv of $((TPP)Fe)_2O(ClO_4)_2$. The signal at 109 ppm is from the pyrrole proton of the oxidizing agent, which is partially converted to monomeric high-spin iron(III) in this reaction.

Examination of the oxidized etioporphyrin I analogue further confirms the assignment of the 50 ppm signal and likewise permits location of the ring-$CH_3$ resonance. Comparison of spectra are made in Figure 4. The oxidized (ETIO)$FeCl^+$ was generated in situ by use of $((TPP)Fe)_2O(ClO_4)_2$ as an oxidizing agent. Partial cleavage of the dimer results in an iron(III) porphyrin pyrrole signal at 109 ppm. The new resonance at 133.1 ppm is approximately 1.5 times as intense as the 50 ppm signal and must represent the ring $CH_3$. Despite the enhanced reactivity of pyrrole-substituted iron porphyrins toward reduction, no large amount of covalent porphyrin modification is apparent. Thus, solutions were brought to room temperature, and the iron porphyrin dissolved in methylene chloride was washed with aqueous HCl solution. The resulting chloroiron(III) porphyrin showed less than 5% modification as judged by minor components present on a thin layer chromatogram.

**Magnetic Measurements.** Solution magnetic measurements were performed at low temperature by the Evans NMR method. One equivalent of imidazole was added to methylene chloride solutions of (TPP(*p*-$OCH_3$))FeCl($ClO_4$) and (OEP)FeCl($ClO_4$). The complete proton spectra as well as the tetramethylsilane reference peaks were recorded. A combination of integration and chemical shift measurements permitted determination of the concentrations of high- and low-spin oxidized and reduced species. The following principles and assumptions were employed, using the spectrum in Figure 1c as an example. Addition of 1 equiv of imidazole converts slightly less than half of the (TPP(*p*-$OCH_3$))Fe(Cl)($ClO_4$ into $[(TPP(p\text{-}OCH_3))Fe(Im)_2]^{2+}$. Areas of far downfield and far upfield pyrrole proton signals show that 44% of the total iron porphyrin is in the bis-ligated product. It is assumed that all of this species is in the oxidized form since, as noted previously, the presence of the high-spin oxidized material serves to keep the bis(imidazole)complex in its oxidized form. The pyrrole peak at 90 ppm represents the averagle for (TPP(*p*-$OCH_3$))FeCl and (TPP(*p*-$OCH_3$)(Cl)($ClO_4$) in the fast electron exchange limit. Limiting values for these two species at −38 °C are respectively 99 and 72 ppm. Hence, from mole fraction weighted averages, only 33% of the 90 ppm peak is made up of parent oxidized porphyrin. The total iron porphyrin composition is now described as 44% low-spin bis(imidazole)iron(III) porphyrin radical complex, 18% parent high-spin iron(III) porphyrin radical, and 38% high-spin iron(III) porphyrin. Measurement of total paramagnetic susceptibility and assumption of $\mu = 5.92\ \mu_B$ for the iron(III) porphyrin and $\mu = 5.5\ \mu_B$ for the high-spin iron(III) porphyrin radical yields a value of $\mu = 2.8 \pm 0.2\ \mu_B$ for the oxidized bis(imidazole) complex $(TPP(p\text{-}OCH_3))Fe(Im)_2^{2+}$. A value of

3.3 ± 0.3 $\mu_B$ was estimated for (OEP)Fe(Im)$_2^{2+}$.

Methylene chloride–toluene (1:1) solutions of (TPP(*p*-OCH$_3$))Fe(Im)$_2^{2+}$ and (OEP)Fe(Im)$_2^{2+}$ were also generated at low temperature in ESR tubes. Spectra recorded at 77 K exhibited minor $g = 6$ signals for high-spin iron(III) and signals for the low-spin bis(imidazole)iron(III) porphyrin complex. Intensities of these signals correspond to only a fraction of the total iron porphyrin present, and it was concluded that the bis(imidazole)iron(III) porphyrin radical species is ESR "silent" at 77 K. No significant sharp free radical signals were detected. Thus, if the iron porphyrin is oxidizing imidazole by a free radical mechanism, rapid radical combination or efficient relaxation of the radical spin must take place.

## Discussion

On the basis of theoretical calculations two metalloporphyrin radical types have been described.[22] The $a_{2u}$ radical exhibits large spin density at meso carbon and pyrrole nitrogen positions, whereas the $a_{1u}$ radical has spin density concentrated at pyrrole carbon positions. Very large phenyl proton NMR shifts are unprecedented for simple paramagnetic metallotetraphenylporphyrins but have been observed for the $a_{2u}$ type radical of oxidized high-spin iron(III) porphyrins.[3,5,6,10,12-15] The very large, alternating phenyl proton shifts for bis(imidazole) complexes of oxidized iron tetraphenylporphyrins must accordingly be attributed to an $a_{2u}$ radical state. Electron spin resonance measurements for the (TPP)Zn(ClO$_4$) $a_{2u}$ radical species indicate an electron-nuclear coupling constant of 0.316 G (0.88 MHz) for the phenyl *o*-proton.[41] This value may be translated into an absolute NMR isotropic shift of 29 ppm at −38 °C by the relationship:[42]

$$\frac{\Delta H^{iso}}{H} = A^H \frac{|\gamma_e|}{|\gamma_H|} \frac{S(S+1)}{3kT} \qquad (3)$$

The calculated 29 ppm value is reassuringly of the same magnitude as the 40 ppm upfield shift observed for the phenyl *o*-proton of (TPP)Fe(Im)$_2^{2+}$.

The most striking difference between high-spin and low-spin iron(III) tetraphenylporphyrin radicals (aside from line widths) is the fact that the signs of phenyl resonances are reversed for the two species. Thus, phenyl ortho- and para-proton signals are far downfield for the high-spin chloroiron(III) species, but shifts are of the same magnitude and upfield for the bis(imidazole) complex. A theoretical description for this reversal phenomenon cannot be offered here. However, at the empirical level it appears that the phenyl shift pattern of the high-spin iron(III) porphyrin radical is the exceptional case and that the pattern for the low-spin iron(III) porphyrin radical parallels in direction the shift pattern of several other recently identified metallotetraphenylporphyin radicals. Thus, a downfield meta signal and upfield ortho and para signals are observed for tetraphenylporphyrin drivatives of the high-spin iron(III) $\mu$-oxo dimer radical,[3] a spin-admixed $S = {}^3/_2, {}^5/_2$ iron(III) radical,[15] a presumed iron(IV) radical,[7] and a copper(II) radical.[43]

An apparent cancellation of approximately two spins (by an incompletely defined mechanism) is observed for high-spin iron(III) porphyrin $\pi$-cation radical species.[6,12] This does not appear to be the case, however, for the analogous oxidized low-spin bis(imidazole) complexes. The solution magnetic moment for a simple low-spin bis(imidazole)iron(III) porphyrin complex is 2.3 $\mu_B$.[44] Assuming the spin-only value for the radical and no coupling between the two $S = {}^1/_2$ centers, the magnetic moment for a low-spin iron(III) porphyrin $\pi$-cation radical is expected to be 2.9 $\mu_B$. This value compares very favorably with magentic moments of 2.8 ± 0.2 and 3.3 ± 0.3 $\mu_B$ estimated in this study for (TPP(*p*-OCH$_3$))Fe(Im)$_2^{2+}$ and (OEP)Fe(Im)$_2^{2+}$, respectively. Furthermore, any antiferromagnetic coupling between metal and radical spins must be relatively small, as the pyrrole proton chemical shift values show no significant deviation from Cuire law behavior. Absence of strong coupling is also suggested for the $S = 1$ iron(IV) and porphyrin radical centers of HRP compound I.[25,26] Although the low-spin iron(III) porphyrin radical complexes are not isoelectronic with compound I, the species do provide a demonstration that strong metal–radical coupling is not a necessity. Lack of metal–radical coupling has also been observed in the solid state for a bis(perchlorate)iron(III) tetraphenylporphyrin radical.[13,14]

Although (ETIO)Fe(Im)$_2^{2+}$ is at the same formal oxidation level as HRP compound II, the radical spin density distribution makes the adduct a more appropriate compound I model. This is most evident in the proton NMR shift patterns. The four porphyrin ring-methyl proton NMR signals have been observed in the downfield region between 50 and 74 ppm for HRP compound I and between 52 and 103 ppm for the deuterohemin-substituted HRP compound I.[30] Ring-CH$_2$ signals for these two oxidized compounds are found in the 20–43 ppm region. For comparative purposes, values at 25 °C calculated for (ETIO)-Fe(Im)$_2^{2+}$, assuming Curie law behavior, are 100 pm (ring CH$_3$) and 39 ppm (ring CH$_2$). The much larger shifts observed for ring–CH$_3$ vs. ring–CH$_2$ residues both for HRP compound I and for the model complex are indicative of $\pi$-spin density in the porphyrin ring. Thus, a freely rotating methyl group can receive $\pi$-spin density from an aromatic center by the hyper-conjugation mechanism[45] much more efficiently than a methylene group which may have a preferred, rotationally hindered orientation. If the paramagnetic shift mechanism was due to a predominant $\sigma$-spin delocalization or dipolar contribution, the ring–CH$_3$ and –CH$_2$ resonances would be shifted by equivalent amounts.

Overall the results for (ETIO)Fe(Im)$_2^{2+}$ provide the best rationalization of radical spin delocalization as dictating the proton NMR spectrum of HRP compound I. Comparable chemical shift values are supportive as noted above. Furthermore, relatively sharp proton signals for the model compound provide reassurance that the radical spin does not necessarily broaden NMR signals beyond detection. The expectation of extreme broadening by a porphyrin radical led to an earlier formulation of HRP compound I as a high-spin iron(IV) porphyrin with the radical localized on a protein moiety.[29] However, relaxation of radical spin by the paramagnetic iron center as indicated by a very broad ESR radical signal[25,26] effectively means that nuclear relaxation will not be excessively short. Recent ENDOR measurements for HRP compound I also provide compelling support for placement of the radical on the porphyrin.[26] Proton ENDOR coupling constants tentatively assigned to porphyrin ring methyl groups should in principle allow direct calculation of proton NMR shift values by eq 3. In terms of chemical shift values, the ENDOR results predict methyl signals from 37 to 157 ppm (at 25 °C), as compared with observed values of 50 to 74 ppm. Perhaps one cannot expect extrapolation of solid-state ENDOR measurements made at 2 K to exactly match ambient solution results. Hindered methyl rotation at low temperature would necessarily induce a larger range of methyl proton coupling constants.

**Acknowledgment.** Support from NSF Grant CHE 79-10305 and NIH Grant GM 28331 is gratefully acknowledged.

**Registry No.** (TPP(*p*-OCH$_3$))FeCl(ClO$_4$), 79623-69-1; (TPP(2,4,6-OCH$_3$))FeCl(ClO$_4$), 87938-42-9; (OEP)FeCl(ClO$_4$), 82963-19-7; (OEP)FeCl(ClO$_4$)-*meso*-$d_4$, 87938-44-1; (ETIO)FeCl(ClO$_4$), 87938-46-3; imidazole, 288-32-4; peroxidase, 9003-99-0.

(41) Fajer, J.; Borg, D. C.; Forman, A.; Dolphin, D.; Felton, R. H. *J. Am. Chem. Soc.* **1970**, *92*, 3451–3459.
(42) Jesson, J. P. In "NMR of Paramagnetic Molecules"; La Mar, G. N., Horrocks, W. DeW., Holm, R. H., Eds.; Academic Press: New York, 1973; pp 1–52.
(43) Godziela, G.; Goff, H. M., submitted for publication.
(44) Goff, H. M. *J. Am. Chem. Soc.* **1981**, *103*, 3714–3722.
(45) La Mar, G. N. In "NMR of Paramagnetic Molecules"; La Mar, G N., Horrocks, W. DeW., Holm, R. H., Eds.; Academic Press: New York, 1973; pp 85–126.